CR 151018

MCDONNELL DOUGLAS TECHNICAL SERVICES CO.
HOUSTON ASTRONAUTICS DIVISION

SPACE SHUTTLE ENGINEERING AND OPERATIONS SUPPORT

1.3-DN-C0304-022

"EVALUATION OF ELECTROSTATIC CHARGE EFFECTS ON THE DATA PROCESSING SYSTEM AND THE ORBITER COMMUNICATION AND TRACKING RECEIVERS

AVIONICS SYSTEM ENGINEERING

---

29 Sept. 1975

This Design Note is Submitted to NASA Under Task Orders No. C0304 and C0308 in Fulfillment of Contract NAS 9-13970.

PREPARED BY: R M Lawton FLS
R. M. Lawton
Senior Engineer
488-5660 Ext. 285

APPROVED BY: L. R. Blanke
L. R. Blanke
Task Manager
488-5660 Ext. 261

APPROVED BY: R F Pannett
R. F. Pannett
WBS Manager
488-5660 Ext. 258

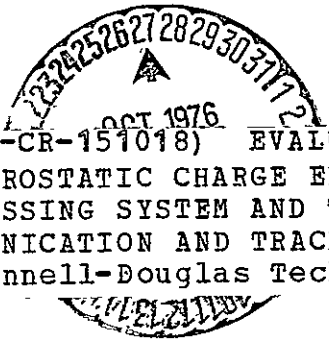

1.0 SUMMARY

The objective of this design note is to present an analysis of radiated interference test results obtained from frictionally charged Orbiter TPS tile. These tests were performed by the MDC, St. Louis, Lightning Laboratory as authorized by Task Order C0308. The tests included the measurement of noise pick-up by Orbiter S-band, L-band, C-band, and Ku-band antennas located beneath the tiles in a manner simulating their installation on Orbiter. In addition, the radiated field characteristics resulting from the static discharge was determined. The results are analyzed as to their effect on data bus equipment and on Orbiter Communications and Tracking (C&T) receivers.

It is concluded that the radiated interference should have no effect on MDM's. However the CPU, IOP and PMU enclosures require some minor modification to assure immunity from P-static interference.

To evaluate the radiated effects on MIA's located in CPU's, IOP's and PMU's, it is recommended that unshielded MIA's used in DBEL testing be subjected to the characteristic radiated spectrum described in this note. This spectrum can be simulated by using a 400 KV Van de Graff generator.

Consideration should be given to performing conducted susceptibility tests on all data bus equipment cables to evaluate P-static effects coupled through system cabling.

Orbiter antenna tests indicate that the S-band receiver should not be affected by P-static noise. The TACAN and Radar Altimeter performance appears to be adequate but with a small margin. MSBLS performance is uncertain because laboratory instrumentation cannot approach the MSBLS sensitivity.

It is recommended that the Radar Altimeter and MSBLS be tested with frictionally charged TPS material.

2.0 DISCUSSION

Reference (1) memo requested MDTSCO personnel to help make the electrostatic discharge tests on the MIA's (Multiplexer Interface Adapters) in the Data Bus Evaluation Laboratory as meaningful as possible. As a result, MDC has conducted tests to determine the radiated interference produced by electrostatic discharges of frictionally charged TPS. Attachment 1 is the test report which completes the effort authorized by Task Order C0308.

2.1 Effects of P-Static Noise on Selected Digital Equipment

The analysis of potential MIA circuit susceptibility must consider the amplitude and spectrum of the radiated noise, shielding effectiveness of the Orbiter skin, shielding effectiveness of the pressurized compartment (for equipment in forward bays), shielding effectiveness of the particular equipment under consideration and response bandwidth of the electronics.

The equipments considered in this paper for potential radiated susceptibility are the Multiplexer/Demultiplexer (MDM), General Purpose Computer (GPC), and PCM Master Units (PMU). Antenna conducted susceptibilities of the R. F. Navigation Aids (MSBLS,

Radar Altimeter, TACAN, and S-band Comm.) are also analysed for Operational Impact of P-static.

2.1.1 P-Static Noise Environment

The noise measurements were made while approximately 5 square inches of TPS material were being frictionally charged with blown dust. It is obvious that the Orbiter internal noise fields will be a function of a larger area than this. An area of 1 square meter is taken as the effective noise generation source for any one equipment. Since the equipment typical distance from the TPS is 1 meter or less, and the free space loss increases rapidly with distance, this 1 square meter noise source is considered to be realistic. The noise level extrapolation from 5 square inches to 1 square meter is accomplished on a Root Sum Square (RSS) basis as follows. Since 5 square inches is the unit area with which the measured spectrum is associated and there are 310 of these unit areas in one square meter,

$$20 \log y = X \text{dB}\mu\text{V/M/MHZ}$$

$$\log y = X/20 \text{dB}\mu\text{V/M/MHZ}$$

$$y = 10^{X/20} \mu\text{V/M/MHZ}$$

$$\text{RSS} = 20 \log \sqrt{(10^{X/20})^2 \cdot 310}$$

$$= 20(X/20) + 20 \log \sqrt{310}$$

$$= X + 25\text{dB}$$

where y is any point on the spectral plot of measured data, in μV/M/MHZ

and X is the same point in db μV/M/MHZ. This then, increases the overall spectral amplitude by 25 db.

A simplifying assumption is made that the P-static radiated field is a uniform field at any point inside the vehicle and the amplitude of the field is equal to the level measured as corrected for $1m^2$ TPS surface and vehicle skin shielding. The Air Force EMC design handbook (Ref 2) in Design Note 5F8 gives the shielding effectiveness of a typical aircraft, for the frequencies up to 100 MHZ, as 30 db. Another 30 db of protection can be assumed in this range for Orbiter equipment in the pressurized compartment (forward avionics bays). MDC experience indicates that for frequencies of 1 GHZ and above, inherent shielding effectiveness is about 10 db.

Figure 1, curve A, is a spectral plot of P-static broadband noise assumed to impinge on equipment in Orbiter forward avionics bays. This plot is 35 db lower than the raw data measurements up to 100 MHZ. This results from adding 25 db for extrapolating the noise source to 1 square meter and from subtracting 60 db for the attenuation of the Orbiter skin and the pressurized compartment enclosure. Above 1 GHZ, Curve A is 5 db higher than the raw data measurements, a result of adding 25 db for the 1 square meter extrapolation and subtracting 20 db for the skin and pressurized compartment attenuation. The curve is interpolated between 100 MHZ and 1 GHZ. The noise level of Curve A will be used for evaluating the shielding effectiveness of certain avionics digital equipment. The equipment considered in this paper are the Multiplexer/Demultiplexer, General Purpose Computer, (GPC) and the PCM Master Unit (PMU).

2.1.2 Equipment Shielding Effectiveness

MDM Shielding Effectiveness

Review of the MDM drawings and discussions with NASA personnel revealed that the enclosure is designed as an EMI type enclosure, with electrical continuity at all seams and joints. Therefore the shielding effectiveness is calculated on the basis of the aluminum structure reflection and absorption losses. From Design Note 5 F1 of Reference (2), the enclosure shielding effectiveness is calculated as follows:

SE = R+A or reflections loss plus absorption loss

$$R = 168 + 10 \log \frac{\sigma}{\mu f}$$

$$A = 3.338 \times 10^{-3} t\sqrt{f\sigma\mu} \quad t = \text{thickness of material}$$

Shielding effectiveness of MDM enclosures was calculated over the P-static spectrum (see Figure 1, curve A). When the noise environment is modified by the MDM enclosure shielding, P-static radiated noise exposure of MDM circuitry is essentially eliminated. This is illustrated in Figure 1, curve B. MDM's in the Aft Avionics bays may be exposed to a level higher than those in forward bays since they will not benefit from the shielding of the pressurized compartment. However the forward area of the vehicle is where the higher frictional charging will occur and therefore should have the worst case field levels. Even if the level in the aft bay were 30 db higher, the MIA inside an MDM should not be exposed to an unaccetpable level.

RADIATED P-STATIC NOISE CURVES

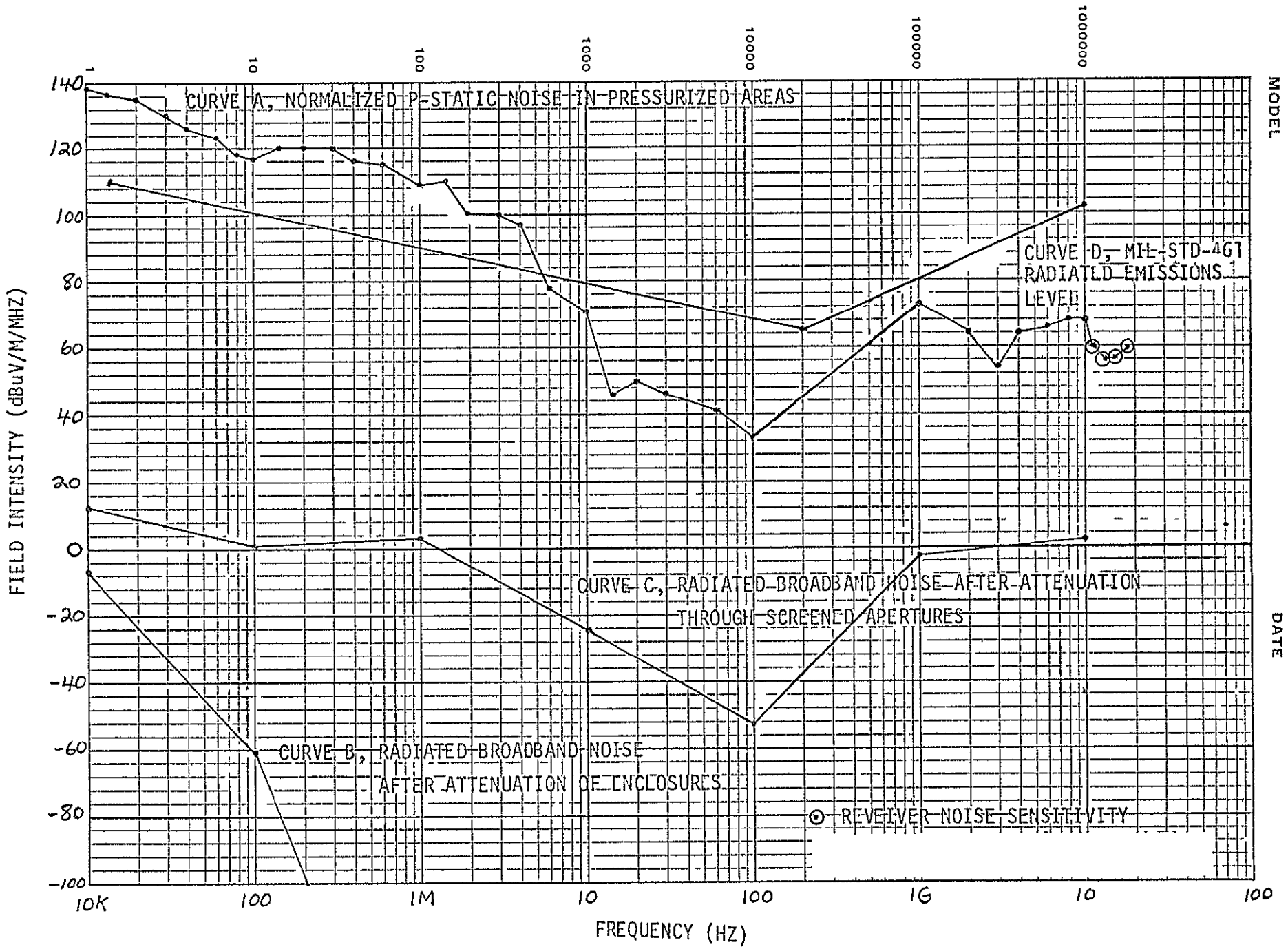

FIGURE 1

221.3 GPC Shielding Effectiveness

The GPC consists of two equipments; Central Processor Unit (CPU) and Input/Output Processor (IOP). These units have very similar enclosures. They are air cooled and have relatively large apertures to external radiated environments. The shielding effectiveness of these enclosures are evaluated by considering the apertures to be waveguides. These enclosures have two rectangular apertures at one end for air intake and one circular aperture at the other end for air exhaust. Enclosure drawings indicate some type of screening across the rectangular apertures but do not give any information on whether the screening material is metallic (designed for EMI shielding) and grounded about it's periphery to the enclosure. The circular aperture has no screening indicated and the air ducting connecting to it is believed to be transparent to radiated fields.

From Design Note 5 F7 of Reference (2), the cut-off frequency of the rectangular aperture (assuming ineffective screen) is

$$fc = \frac{5900}{b} = \frac{5900}{5.3} = 1.11 \text{ GHz}$$

where b is the longest transverse dimensions in inches. Above this frequency the enclosure is essentially unshielded from external radiated environments. At frequencies below $\frac{fc}{10}$ the attenuation may be calculated as

$$A = 27.3\ L/b = 27.3\ (.5/5.3) = 2.58 \text{ db}$$

where L is length of the waveguide in inches. These calculations

indicate that, in effect, the CPU's and IOP's are exposed to the full P-static radiated environment shown in the spectral plot of curve A, Figure 1. This level might interfer with a MIA mounted inside the GPC.

If all the apertures were covered with good EMI screening and if the screening were properly grounded to enclosure structure, the CPU's and IOP's would benefit by the reflection loss effects of the screen. The absorption losses would be neglible. Reflection loss is calculated from:

$$R = 168 + 10 \log \frac{\sigma}{\mu f}$$

Figure 1, curve C is a plot of the resulting noise field impinging on CPU and IOP electronic circuitry after attenuation of curve A by the screening reflection loss. This is a level that the electronics in the CPU and IOP should tolerate since it is well below the radiated emissions levels allowed by MIL-STD-461 as can be seen in Figure 1.

2.1.4 PMU Shielding Effectiveness

Review of the PMU enclosure drawings indicates that the enclosure design has not been optimized for EMI shielding. The surface treatment for cover to case interfaces is per MIL-C-5541, class 1A. This is not a conductive finish and, in effect, creates an aperture

at the case/cover interface for radiated fields. When the waveguide below-cutoff analysis is applied:

$$fc = \frac{5900}{3} = \frac{5900}{3} = 1.97 \text{ GHz}$$

where b - longest dimension between cover mounting screws.

Attenuation for frequencies below fc/10 is:

$$A = 27.3 \left(\frac{L}{b}\right) = 27.3 \left(\frac{.23}{3}\right) = 2.09 \text{ db}$$

where L is the length of waveguide (distance across cover flange). These results indicate that the PMU is essentially unshielded from P-static radiated fields. This problem could be easily overcome by changing the cover/case interface finish treatment to a conductive finish such as MIL-C-5541, Class 3. This would result in the same attenuation as calculated for MDM in paragraph 2.2.1.

2.1.5 P-Static Noise Coupling Through Vehicle Wiring

Another mode of entry for P-static noise into equipment is through wiring entering the equipment enclosures. Pick-up on vehicle wiring can be calculated but the wire shielding effectiveness and coupling modes into internal circuitry are difficult to evaluate. These effects can best be evaluated by test. Common mode and differential mode conducted noise tests are planned for the Data Bus/MIA tests in the DBEL Lab per Reference (3) test plan. These tests will not determine the noise coupling but will determine the effects the cable noise will have on the MIA.

2.2 Proposed Laboratory P-Static Test Method

Reference (1) requested suggested methods of performing tests to evaluate the effect of the static discharge of the TPS. Attachment 1 shows a comparison between the TPS noise measured at one meter away from the test sample and the noise measured one meter away from a 400 KV Van de Graff generator while discharging a six inch arc. This comparison shows the generator to be a good simulation of the noise of the discharging TPS. Therefore, the Van de Graff generator can be used as a noise source in laboratory tests. However, the attenuation of the vehicle skin, the distance between the TPS and the location in the vehicle of the equipment to be tested, and the extrapolation of the noise from a 5 square inch area of test TPS to a larger area on the vehicle (which was described in paragraph 2.1.1) must be taken into account in determining how far away the generator should be placed from the equipment under test.

2.3 Effects of P-Static Noise on C&T Receivers

The results of TPS P-static tests presented in Attachment 1 show that the noise levels received by the antennas are well above the receiver sensitivities. Utilizing the noise data from Attachment 1, the ground to Orbiter RF links were analyzed to determine the effect of noise on the operation of the receivers.

Table I and II shows the nominal Circuit Margin Summary for the RF Links in question.

TABLE 1

CIRCUIT MARGIN SUMMARY

PARAMETER	GROUND-SSO RF LINK S-BAND PM (POST BLACKOUT) TDM	RANGING
1. Ground Transmit Power, dBm	50.0	50.0
2. Ground Transmit Antenna Gain, dB (includes Xmit Loss & Pointing Loss)	34.0	34.0
3. Ground EIRP, dBm	84.0	84.0
4. Space Loss, dB	-156.3 ①	-156.3 ①
5. Polarization Loss, dB	-0.5	-0.5
6. SSO Receive Antenna Gain, dB	-1.0	-1.0
7. SSO Receive Circuit Loss, dB	-5.1	-5.1
8. Total System Losses, dB	-162.9	-162.9
9. Total Received Power, dBm	-78.9	-78.9
10. SSO System Noise Temperature, dB-K	32.5	32.5
11. Boltzmann's Constant dBm/K-Hz	-198.6	-198.6
12. SSO Noise Spectral Density dB w/Hz	166.1	166.1
13. Total Received Power/Noise Spectral Density (Prec/No), db-Hz	87.2	87.2
14. Bit Rate BW (72 KBPS), dB-Hz	48.6	
15. Modulation Loss, dB	-3.3	-11.0
16. Bit Rate (dB-Hz-dB) w/o loss	-51.9	
17. SNR in Bit Rate BW (Eb/NO), dB	+35.3	
18. Theoretical Eb/No, db	8.4	
19. Bit Sync Degradation, db	-1.5	
20. Postdetection Tone Subcarrier Power/ Noise Spectral Density (Psc/N) dB-Hz	9.9	76.2
21. Required (Psc/N)-dB-Hz		55.0
22. Circuit Margin, dB	25.4	21.2

① Utilizes 2106.4 MHZ & 400 N.M.

TABLE 1 (cont.)

CIRCUIT MARGIN SUMMARY

PARAMETER	GROUND-SSO RF LINK	
	TACAN DME	MSBLS DME
1. Ground Trasnmit Power, dBm	64.8	63.0
2. Ground Transmit Antenna Gain, dB (includes Xmit Loss & Pointing (Loss)	4.0	20.0
3. Ground EIRP, dBm	68.8	83.0
4. Space Loss, dB	-148.9 (2)	-141.6 (3)
5. Precipitation Effect, dB(10mm/HR)		-9.0
6. Fading Loss	-2.0	
7. SSO Receive Antenna Gain, dB	0	9.0
8. SSO Receive Circuit Loss, dB	-4.8	-3.0
9. Total System Losses, dB	-155.7	-144.6
10. Total Received Power, dBm	-86.9	61.6
11. Required Minimum Received Signal Power, dBm	-94.0	-77.0
12. Circuit Margin, dB	7.1	15.4

(2) Utilizes 1215 MHZ & 300 M.N.

(3) Utilizes 15550 MHZ & 10 M.N.

TABLE II

CIRCUIT MARGIN SUMMARY

RADAR ALTIMETER

TRANSMIT POWER	(PT)	=	100 WATTS
TRANSMIT/RECEIVE ANT GAIN	(G)	=	10 dB
WAVELENGTH	(λ) λ	=	0.07 M (4285 MHz)
TRANSMITTED PULSEWIDTH	(τ)	=	60 nsec (Min)
ALTITUDE	(H)	=	.76 KM
CABLE LOSS - TWO WAY	(L)	=	-6 dB
SCATTERING COEFFICIENT	(σo)	=	-15 dB
RECEIVED POWER	(Pr)	=	-76 dBm
RECEIVER SENSITIVITY		=	-83 dBm
PROPAGATION VELOCITY		=	+84.6 db - 10 log $3X10^8$ M/sec
MARGIN @2500 FT		=	+7.0 db

$$Pr = \frac{PT\ G^2\ \lambda^2\ C\ \tau\ \sigma o}{64\ \pi^2\ H^3\ L}$$

In order to evaluate the effect of the P-static, the noise level measured using the appropriate antenna (see Table III) was used as the receiver sensitivity and the range at which this noise level plus 10 db (for a signal plus noise to noise ratio of 10 db as specified for the receiver) was overcome by the received signal was calculated. These calculations resulted in the following information:

a) S-Band

Total receiver power @ 400 N.M.	=	78.9 dbm
Required power for (S+N)/N of 10 db	=	-61 dbm
Range db difference	=	17.9 db

Circuit margin from Table I = 25.4 dB > Range difference (17.9 db) therefore S-Band range as affected by P-static is greater than 400 Nautical Miles. Both S-band PM channels have sufficient circuit margin to overcome the P-static noise and provide good data from 400 n.mi. to touchdown.

b) TACAN

Total received power @ 300 N.M.	=	-89.9 dbm
Required power for (S+N)/N of 10 db	=	-64 dbm
Range db difference	=	22.9 db
Distance factor of free space loss @300 N.M.	=	20 log 300
		= 49.5 db
	less	22.9 db
20 log X		= 26.6 db

TACAN Range affected by P-static = X=21.5 N.M.

In order to overcome P-static noise at L-band and provide a 0 db circuit margin, the TACAN range is reduced to 21 n.mi. This range corresponds to an altitude of approximately 46,000 ft. Since P-static noise will not occur above 50,000 ft. it will only affect the TACAN between the two altitudes or for about 30 seconds. This should not be a problem.

c) Radar Altimeter

Total Received power @2500 ft ($7.6X10^{2}$M) = -76 dbm

Required power for (S+N)/N of 10 db = -54 dbm

altitude difference = 22 db

Distance factor from Table II = 30 log ($7.6X10^{2}$)

= 84.6 db

-22 db

64.4

30 log X = 64.4

log X = 2.147

Altimeter Range as

Affected by P-static $X = 10^{2.147} = 140M \equiv 460$ ft

To maintain a 0 db circuit margin for the Radar Altimeter C-Band link in the presence of P-static noise, the effective operational altitude is reduced to approximately 460 feet. This should not be a problem since present plans do not require reliance upon this data above 400 feet.

As can be seen from Table III the laboratory test equipment was not sensitive enough to read any P-static interference through the Ku-band antenna. However, if that minimum sensitivity (-40 dbm) is assummed to be a noise level, than from Table 1;

	without rain effect	with rain effect
Total received power @10 N.M. slantrange =	- 61.6 or	-52.6 dbm
Required power for (S+N)/N of 10db = (-40+10) =	-30	-30
Range Difference	31.6	22.6

Distance factor free space loss @10 N.M. = 20 log 10 = 20 db

20 db	20 db
-31.6	-22.6
-11.6	-2.6

20 log X = -11.6 20 log X = -2.6

MSBLS range as affected by P-static =

$X = 10^{-.64} = .229$ N.M. with rain effect

$X = 10^{-.13} = .741$ N.M. without rain effect

These results indicate the laboratory results may mask a significant problem with MSBLS.

3.0 CONCLUSIONS AND RECOMMENDATIONS

3.1 Equipment Susceptibility

In evaluating the effects of P-static radiated interference on data bus equipment, it can be concluded from the analysis that:

a) The radiated interference should have no effect on the MDM's unless it is picked up on the cables and transmitted into the MDM.

b) The CPU, IOP and the PMU enclosures are open to radiated interference and could possible be affected by P-static interference. Slight modifications to the case designs (adding screens across ventilation openings and making mating surfaces conductive) can eliminate this possible problem.

c) The MIA's in DBEL test should be subjected to the radiated spectrum shown in curve A of Figure 1 and the spectrum simulated by using a 400 KV Van de Graff generator.

Based on these conclusions the following recommendations are made:

a) Consideration should be given to performing conducted susceptibility tests on all MDM, CPU, IOP, and PMU cables similar to the tests planned for the data bus/MIA tests in the DBEL. These tests should be performed using short duration, fast rise time pulses to evaluate the effect of P-static noise picked up on cables. A possible location for these tests would be the JSC/EG Laboratory.

b) Tests for radiated susceptibility to P-static noise impulse fields should be conducted using the Van de Graff generator as an addition to RF susceptibility tests planned for the GPC, and PMU equipment.

c) Properly bonded screens should be put across the ventilation opening on the CPU and IOP and the mating surfaces of the PMU should be made conductive. This would protect the equipment from other radiated noise sources as well as significantly reduce P-static vulnerability.

3.2 C and T Receivers

The following conclusions can be made from the analysis of the effect of P-static on C and T receiver operation during launch and landing:

a) P-static radiated interference should have no effect on the operation of the S-band receiver.

b) P-static noise may affect the operation of the TACAN but only between 50,000 feet and 46, 000 feet which should not significantly impact mission performance.

c) P-static noise will probably reduce the effective operational altitude of radar altimeter from 2500 feet to 460 feet. This may result in marginal mission performance although the altimeter is not independently relied on above 400 feet.

P-static effects on the MSBLS are uncertain because laboratory receivers cannot approach the MSBLS sensitivity. Based on these conclusions the following recommendations are made:

a) Tests should be performed to further evaluate the effect on the MSBLS using the MSBLS antenna and receiver in the presence of signal and P-static noise.

b) Tests should be performed on the Radar Altimeter using the altimeter and its antenna because the calculations show the altimeter will be affected to an extent where there is not much safety margin left.

4.0 REFERENCES

1. NASA Memorandum from EG/Chief to EJ/Chief, Subject "Data Bus Sensitivity to Electrostatic Discharge" dated 24 January 1975.

2. "AFSC Design Handbook", Series 1-0 General, AFSC DH 1-4 Electromagnetic Compatibility, Third Edition dated 5 January 1975.

3. DBEL Test Plan

Table III

ANTENNA NOISE TEST DATA AND SHUTTLE RECEIVER SENSITIVITIES

Antenna	Frequency (GHZ)	Gain (dB)	Noise Measured With 5 MHZ Bandwidth (dBm)	Radiated Field Interference (dbuV/M/MHZ)	Specified Sensitivity Of Receiver (dBm)
L-Band	1.0	3	-67	73	-90
	1.2	3	-67	70	
S-Band	1.78	6	-69	65	-121 to acquire
	1.94	6	-73	64	
	2.1	6	-71	63.5	-131 for tracking
C-Band	4.4	10.5	-65	66	-80
Ku-Band	15.7	10.5	Below Test Receiver Sensitivity	57	-74

1.3-DN-C0304-022
Attachment 1

Copy number

Report number MDC A3673

TPS ELECTROSTATIC CHARGE EFFECTS ON AVIONICS SYSTEMS AND ANTENNAS

FINAL REPORT

Revision date

Revision letter

Issue date 24 September 1975

Contract number

Prepared by M B Munsell

M. B. Munsell
Laboratory Engineer

Approved by D W Clifford

D. W. Clifford
Unit Chief

MCDONNELL AIRCRAFT COMPANY

Box 516, Saint Louis, Missouri 63166 – Tel (314)232-0232

MCDONNELL DOUGLAS

ABSTRACT

The purpose of this test program was to provide information on the electromagnetic radiation characteristics of streamering discharges produced by triboelectric (frictional) static charge buildup on the Space Shuttle LI-1500 TPS. A blown-dust static charge generator was employed to produce triboelectric charging on a simulated Space Shuttle TPS panel. Charging rates measured were as much as 10 times higher than those which have been measured on conventional aluminum skinned aircraft in flight. The field intensity of the electromagnetic radiation from static discharge streamering on the tiles was measured in order to evaluate potential interference with digital logic circuits in the Shuttle. Also typical full-scale Shuttle C-band, L-band, S-band, and Ku-band flush antennas were realistically mounted on the underside of the TPS panel and the levels of RF interference coupled into the antennas were measured.

The field intensity measurements revealed interference levels much higher than had been previously measured over a major portion of the frequency range from 14kHz to 10GHz. The levels of RF interference coupled into the C-band, L-band, and S-band antennas were higher than the minimum receiver sensitivities of their respective Shuttle receivers (as much as 50 dB in the case of the S-band antenna). Due to these results a potential P-Static problem is indicated.

1. INTRODUCTION. The purpose of this test program was to provide information on the electromagnetic radiation characteristics of streamering discharges produced by triboelectric static charge buildup on Space Shuttle TPS panels. This program was designed to assist JSC in the evaluation of static charge effects on Shuttle Avionics Systems and Antennas by providing a basis for simplified generation of P-Static type noise and by characterizing the response of selected antennas to P-Static noise. The tests were conducted by the McDonnell Aircraft Company's Lightning Simulation Laboratory in St. Louis, using a blown-dust static charge generator to produce triboelectric charging on a 7-tile LI-1500 TPS panel.

Triboelectric charging currents were measured for the TPS panel as well as for individual samples of TPS, polyurethane, fiberglass, plexiglass, quartz, aluminum and other materials characteristic of conventional aircraft. The free-field electromagnetic radiation from streamering on the TPS panel was measured in order to evaluate potential interference with digital logic circuits. These field intensities were compared with the measured radiation from a small 400kV Van de Graff generator which could be easily set up in any avionics lab for the purpose of conducting equipment susceptibility tests. In addition, typical full-scale Shuttle C-band, L-band, S-band and Ku-band flush antennas were realistically mounted under the TPS tiles and the streamer-generated RF interference at the antenna terminals was measured. These noise levels were compared to the minimum sensitivities of the Shuttle receivers to determine if receiver degradation could be anticipated.

2.0 DESCRIPTION OF TEST ARTICLES

2.1 TPS PANEL. The tests were conducted by blowing Wondra flour on a test panel simulating the actual TPS tile and antenna installations. Photographs of the panel are shown in Figures 1 and 2. LI-1500 tiles, 15.2 cm on a side and 3.2 cm thick, from a previous test program were mounted along with the 0.406 cm thick Nomex felt Strain Isolation Pad (SIP) in a representative 7 tile array on an aluminum baseplate (45.7 x 45.7 x 0.318 cm). Continuous 0.025 cm thick RTV 560 bonds were used at the tile/SIP and SIP/baseplate interfaces. The baseplate included a cutout for mounting the selected antennas.

2.2 TPS TILE SIMULATION. In order to produce the most realistic static charge behavior, the LI-1500 tiles were adjusted for the proper thickness over the antennas by incorporating an additional thickness of (simulated) tile material between the existing undercut TPS tiles and the SIP. Since the electrical characteristics of the TPS coating and the distance from the top surface of the tile to the metal baseplate are the primary factors which determine the length and intensity of the streamering, the nature of the simulated tile extension was important only in so far as the surface flashover characteristics were concerned; the bombarding particle stream did not penetrate the joints to contact the extensions to any significant degree. Therefore, flashover tests were conducted on a number of candidate simulation materials, including polyurethane foam, fiberglass, plexiglass and phenolic for comparison with flashover characteristics of the TPS coating. Flashover characteristics of clean dielectric surfaces are primarily a function of the microscopic structure of the material and of the propensity of the material to absorb moisture. However, in practical applications, contamination of the surface by common atmospheric pollution often overshadows the basic characteristics of the material. For the comparison tests, however, clean materials were used under controlled humidity conditions. The following is a tabulation of the relative flashover voltage measured, showing that plexiglass has very nearly identical flashover characteristics to the TPS.

FLASHOVER VOLTAGES OF CANDIDATE SIMULATION MATERIALS

Material	Voltage Required to Flashover Specified Length of Surface (kV)			
	1.27 cm	2.54 cm	3.81 cm	5.08 cm
TPS (LI 1500)	18	34	44	55
Plexiglass	18	33	46	55
Phenolic	16	25	33	43
Fiberglass	18	31	40	50
Polyurethane (coated)	18	28	38	45

The LI-1500 tiles on hand were 3.2 cm thick, undercut 1.9 cm around the lower half. The thickness of tiles to be used over the L-band, C-band, S-band and Ku-band antennas on the Shuttle varies from 0.56 to 8.26 cm, as seen from the following table.

Antenna	TPS Thickness (cm)	Configuration
Ku-Band (MSBLS)	2.97	Waveguide
S-Band Lower	8.26	Cavity-Backed Helix
Upper	0.89	Cavity-Backed Helix
C-Band (Altimeter)	5.41 to 5.82	Cavity-Backed Helix
L-Band (TACAN)	0.56 to 5.21	Annular Slot

Much of the concern over P-Static interference is focused on the L-band TACAN antenna. Since the maximum thickness over the TACAN is approximately centered between the extremes listed in the table, the tile thickness on the panel was set at 5.21 cm. The construction of the tiles showing the addition of the plexiglass extensions can be seen in Figures 1 and 9.

2.3 TILE ORIENTATION. The orientation of the tiles over the antennas may influence the antenna response to the radiation. For this test, no attempt was made to determine the relative tile/antenna orientations for the four antennas tested, since each antenna installation on the Orbiter (even of the same type) will probably have a different tile configuration over it. It was assumed that having a gap across the center of the receiving area is worst case, since

streamering will occur in the gaps and the closest coupling is possible in that situation. Worst case representative conditions were therefore approximated as much as possible.

2.4 ANTENNA MOUNTING. The panel baseplate was fabricated from 0.318 cm thick aluminum cut out to accept the TACAN antenna, which was the largest of the 4 antennas tested. Separate adapter plates were fabricated for the other 3 antennas to allow them to be mounted in the same cutout. Each antenna baseline mounting configuration was duplicated as closely as possible to maintain an accurate simulation. The Ku-band antenna was mounted flush with the top surface of the aluminum baseplate. The other three antenna installations incorporated a honeycomb carrier panel and a Moisture Avoidance Pad (MAP) between the SIP and the antenna. The carrier panel was fabricated from 0.95 cm thick phenolic impregnated fiberglass honeycomb with two face sheets of .025 cm thick polyimide impregnated fiberglass fabric bonded to each side with FM-123 adhesive. The MAP consisted of a 0.160 cm thick sheet of RTV 560. Photos of the antennas and installations are shown in Figures 3 thru 7.

3.0 TEST SETUP AND PROCEDURE

3.1 FRICTIONAL CHARGE SIMULATION. The P-Static Blown Dust Simulator was employed to generate a stream of high velocity dust particles (Wondra Flour) to impact a test specimen causing triboelectric charging of the surface. Several other investigators have used this same general type of apparatus to simulate P-Static effects. Almost all have reported erratic charging rates or inconsistent RF noise generation. It was felt that these problems were associated with agglutination and uneven flow of particles caused by moisture and oil found in typical air sources. Therefore, dry high pressure nitrogen gas (generated from a 15,000 gallon LN_2 tank) was utilized as the accelerating medium. This resulted in very uniform charging and RF noise generation. Also the chamber was equipped with a filtered exhaust system to minimize the possibility of the formation of a cloud of charged particles while operating.

During the test setup the particle stream was directed onto an aluminum panel at four incident angles of impingement (15, 30, 45 and 60 degrees). The highest charging current was obtained at 45 degrees and consequently this impingement angle was used for all testing. The flux, velocity, and diameter of the particle stream were adjusted to obtain a charge rate of 220μ amps/m^2 (20μ amps/ft^2) on the aluminum panel, which is about one-half the worst case cahrging rate observed on conventional aircraft in flight. It was determined that these test conditions would not seriously erode the TPS test panel over the duration of the test and therefore these parameters were adopted for all charging current and radiated noise measurements. A particle velocity of approximately 120m/sec (400 ft/sec) resulted. This is representative of the Orbiter air velocity at P-Static altitudes. The impact area of the particle stream was 32 cm^2 (5 in^2). Photographs of the test setup are shown in Figures 8 and 9.

3.2 CHARGING CURRENT MEASUREMENTS. A Hewlett-Packard 425A Microammeter was used for monitoring the charging currents by grounding the specimen through

the microammeter and recording its output on a strip chart recorder. Charging currents were measured for the TPS panel as well as for individual samples of TPS, polyurethane, quartz, aluminum, fiberglass, plexiglass, phenolic, window glass, pyrex, and titanium. Current measurements on dielectric samples were measured by mounting them on an aluminum baseplate and measuring the current flowing between the aluminum plate and ground. In the case of the multiple-tile TPS panel, the charging current measured was the total current flow from ground to the metal baseplate. By measuring the charging current at the aluminum baseplate, the total mechanism of charge buildup on the tiles and streamer discharges down the sides of the panel and through the SIP was included. In order to insure that all of the measured charging current was coming from the direct impingement of the blown dust stream and not from the secondary impact of any particles circulating about the chamber, a grounded 15.2 cm square metal collector plate was placed on the surface of the TPS panel to intercept the main stream of particles. The small remaining current measured to the TPS panel baseplate was then used to correct the charging rates measured on the tile panel.

3.3 RADIATED NOISE MEASUREMENTS. Field intensity measurements of the radiated-emissions from the streamering on the TPS panel were conducted over the frequency range of 14 kHz to 18 GHz. The particle stream was directed at the "T-joint" centered over the antenna cutout as shown in Figure 9. For these tests the cutout was filled with an aluminum disk having the same thickness as the baseplate. Both grounded and floating panel configurations were used. In the first condition the baseplate of the TPS panel was grounded through the microammeter. In the second case the microammeter was disconnected from the baseplate allowing the entire panel to charge up to a high potnetial. The microammeter was then connected as the ground link to another aluminum sheet mounted 6.4 cm below the baseplate and parallel to it. This configuration thus produced corona current from the main panel to the ground plate.

The EMI measuring equipment that was used to measure the radiated noise at the various frequencies is listed in Table 1. Because the anticipated EMI sensitive avionics use pulse and digital circuits, the peak intensity of an emission as a function of frequency per unit bandwidth becomes the most important measure of potential EMI. Also, since MIL-STD 461A has its limits based on peak values, the peak detector function of the test instrument was used when available (from 14 kHz to 10 GHz). The distance from the test article to the antenna was standardized at one meter.

The radiated noise level from a small 400 kV Van de Graff generator was measured in the same manner as the TPS panel. It was hoped that its radiation caharcteristics would allow it to be used to simulate P-Static noise for checking the susceptibility of avionics systems in the lab. The Van de Graff was discharged to a 5.1 cm diameter sphere at distances of 7.6 and 15.2 cm as shown in Figure 10.

3.4 ANTENNA RF NOISE TEST. The C-band, L-band, S-band, and Ku-band Orbiter antennas were mounted in turn on the underside of the TPS panel as previously described. The particle stream was again directed at the "T-joint" centered over the antenna cutout. The antenna output was connected directly to the appropriate test instrument and the level of RF interference coupled into each antenna was measured around its design frequency. The EMI measuring equipment used for this test is also listed in Table 1.

4.0 TEST RESULTS AND DISCUSSION

4.1 CHARGING CURRENT MEASUREMENTS. The charging currents and equivalent charging rates obtained for each material are listed in Table 2. Charging rates as high as 430μ amps/m^2 (40μ amps/ft^2) have been measured on conventional aluminum skinned aircraft in flight. For this test program an equivalent charging rate of 220μ amps/m^2 on aluminum was used. Under these conditions the simulated Shuttle TPS panel exhibited a charging rate approximately 10 times higher than aluminum, indicating a potential worst-case charging rate in flight of 4300 μamps/m^2 (400μ amps/ft^2). The quartz material scheduled for Orbiter windows had a charging rate about twice that of ordinary window glass and over 10 times that of plexiglass. Extrapolating these results to a full-scale Orbiter is difficult because of variations in the TPS configuration over the surface of the vehicle (portions of the frontal area incorporate different materials). In addition the angles of particle impingement, particle size and density, total charging area, etc. cannot be predicted over the operational life of the Shuttle. It is known that on conventional aircraft dielectric surfaces no larger than a windshield or canopy have proven very troublesome. Due to the fact that essentially the entire surface of the Orbiter is non-conducting and the TPS charging rates are far in excess of conventional materials, the possibility of a significant P-Static problem cannot be reasonably discounted.

The coated polyurethane, to be used on the early flight vehicles, presented a low charging rate initially but increased continuously during a one-minute exposure. Coating erosion was observed after the test. A slight difference was observed between the TPS panel and TPS single tile charging rates. This was probably due to the fact that the particle stream was impinging onto a "T-joint" on the panel vs a flat surface on the single tile. Also, the single tile had been used for previous blown dust tests and appeared to have a smoother surface. All materials except polyurethane and fiberglass had negative charging currents indicating a negative charge buildup due to the triboelectric charging

with Wondra flour.

4.2 RADIATED NOISE TESTS. The free-field intensity data obtained from the blown dust and Van de Graff tests is presented in Table 3 and is shown graphically in Figure 11. The interference levels generated from the streamering on the TPS panel were much higher than those measured previously over a major portion of the frequency range from 14 kHz to 10 GHz. At 14 kHz the field intensity was about 170 dBμV/m/MHz and at 1 MHz (Shuttle Data Bus Frequency) it was about 140 dBμV/m/MHz. Visual observation with an oscilloscope connected to the video output of the receiver at 1.5 MHz indicated fairly consistent pulse peaks with a pulse repetition rate on the order of 10 PPS.

Surprisingly high field intensities (about 60 dBμV/m/MHz) were still being generated in the 1 to 10 GHz range, the domain of the L-band, S-band, and C-band antennas and receivers. Measurements above 1 GHz utilized linearly polarized standard gain horn antennas. At 1.94 GHz the vertical component of the emission was about 20 dB higher than the horizontal component. Vertical polarization was therefore used because that alignment detected the maximum component of the radiated noise. The pulse peaks at 1.94 GHz were not of uniform amplitude, and the repetition rate could not be determined visually with an oscilloscope. However, switching detector functions on the receiver indicated that the repetition rate was less than 30 PPS, at least for the high amplitude pulses.

Measurements from 12.4 to 18 GHz did not reveal any noise above the ambient level. However, the receiver used had no peak detector function and does not respond well to low repetition rate signals.

Again it is difficult to project these results to the Orbiter. However, it seems reasonable to assume that if larger areas of LI-1500 TPS (quantitatively representative of Orbiter frontal area) were subjected to P-Static conditions, the field intensity levels generated would not be appreciably lower than those observed in this test. They might, in fact, be higher if larger TPS tiles or

panels are used. Also the pulse repetition rate would very likely increase with area and could easily approach thousands of pulses per second in an area with a radius of one meter.

The field intensities generated by the Van de Graff discharging across an air gap of 15.2 cm were slightly higher but still in good agreement with the blown dust levels as a function of frequency from 14 kHz to 15 MHz. From 15 MHz to 1 GHz the levels become somewhat less consistent at a given frequency and appear to cycle about the blown dust data as a function of frequency. Above 1 GHz the noise level at the 15.2 cm discharge distance dropped considerably below that of the blown dust. When the discharge distance was decreased to 7.6 cm,spark discharges occurred at the rate of approximately one per second. During these discharges, peak levels increased to roughly those of the blown dust from 2 to 10 GHz. Above 10 GHz no noise above ambient was detected for the same reasons previously mentioned.

From 14 kHz to 15 MHz the Van de Graff would appear to be a very good simulator for the peak field intensity emanating from TPS under blown dust conditions. The field levels could be adjusted downward slightly, to coincide with those of the blown dust, by increasing the distance from the Van de Graff to the avionic system under test. Since little is known about the mechanisms causing digital circuit upset and interference, the role of the very high frequency radiation is uncertain. However, the Van de Graff could reasonably be utilized for equipment level susceptibility tests. After the correction of any problems identified by the Van de Graff, final evaluation of the avionics could be conducted with the frictional charging apparatus.

4.3 ANTENNA RF NOISE TEST. The levels of RF interference coupled into the four antennas and the minimum sensitivities of their respective Shuttle receivers are listed in Table 4. The noise levels measured on the antenna terminals were significantly higher for the C-band, L-band, and S-band antennas than their respective receiver sensitivities. These values do not relate

directly because of the operational characteristics of the Shuttle receivers. However, even without extrapolating to a larger charging area or worst case conditions, the noise levels are as much as 50 dB higher than the receiver sensitivity. This result strongly suggests the probability of an operational problem.

No noise above ambient was seen at the Ku-band terminals; however, the test receiver was not as sensitive as the Shuttle receiver is, so it cannot be guaranteed that interference-free operation will be experienced.

5.0 CONCLUSIONS AND RECOMMENDATIONS

The very high charging rates experienced by the LI-1500 TPS (compared to conventional aircraft materials), the high free-field intensities generated over the entire frequency range of the test, and the levels of RF interference coupled into the Shuttle antennas, all indicate a potential P-Static problem on the Shuttle, even for atmospheric conditions well below worst case. It is reiterated that only a small portion of a sub-size panel was subjected to triboelectric charging in this test. It is recommended that further studies be conducted to determine the susceptibility of the Shuttle receivers to this type of interference. Depending upon the results of such tests and an analysis of the vulnerability of the Shuttle data bus and computers, it may be necessary to consider the development of surface charge bleed-off techniques or circumvention measures for the affected avionics circuits. In the latter case, a technique is required to evaluate the response of the full-scale operational vehicle to TPS P-Static interference.

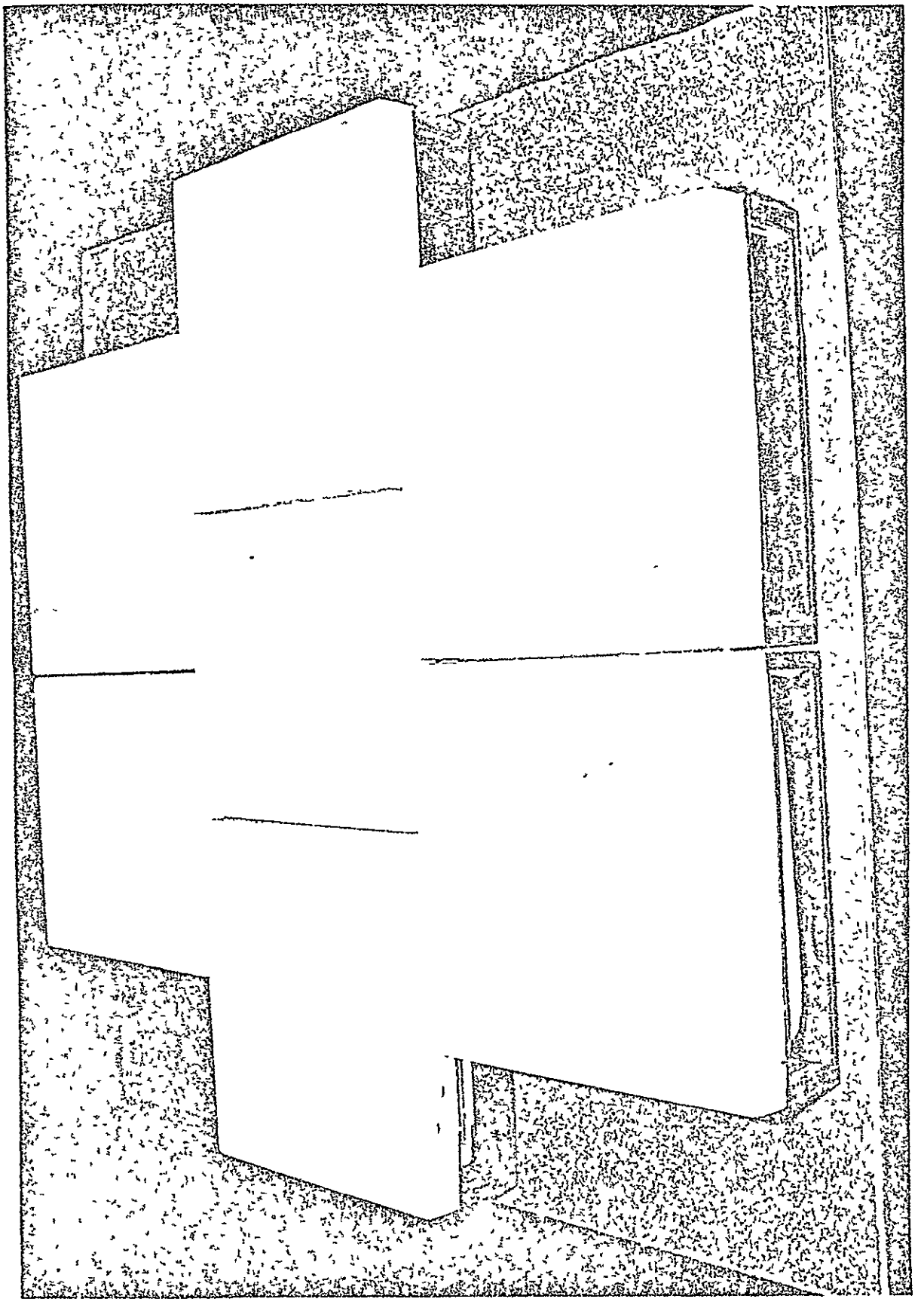

FIGURE 1 - TOP VIEW OF TPS PANEL

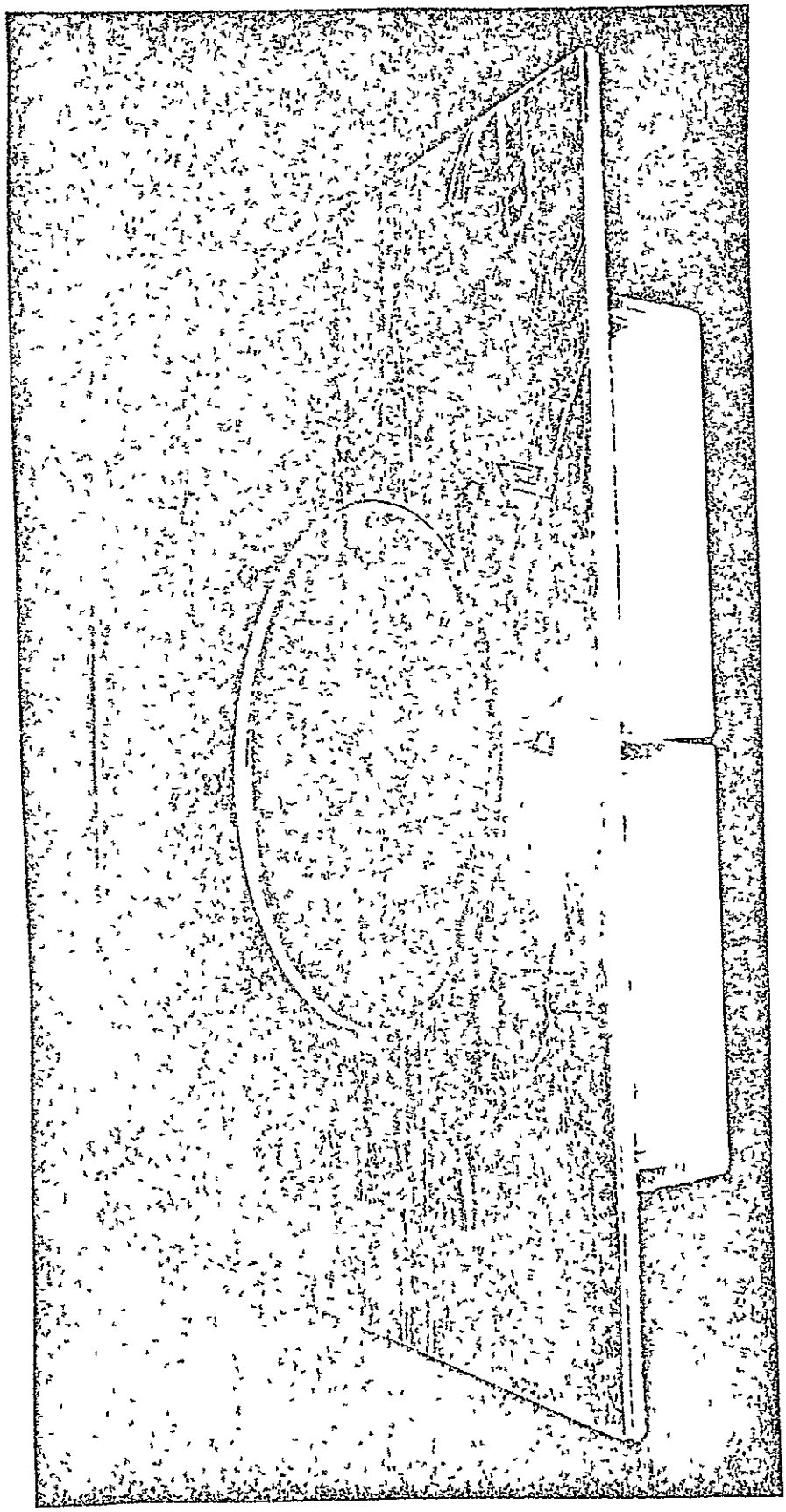

FIGURE 2 - BOTTOM VIEW TPS PANEL

FIGURE 2

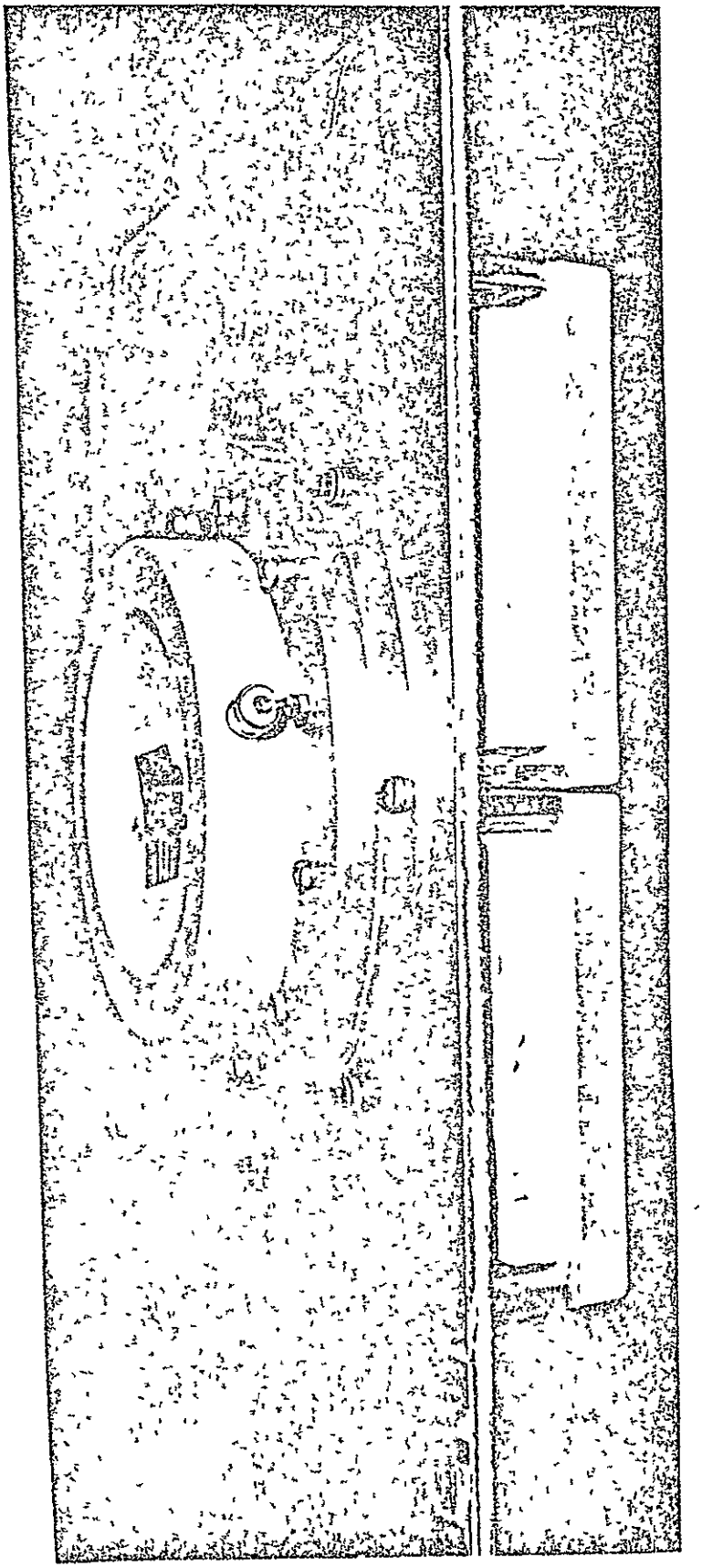

FIGURE 3 - TYPICAL ANTENNA INSTALLATION ON TPS PANEL

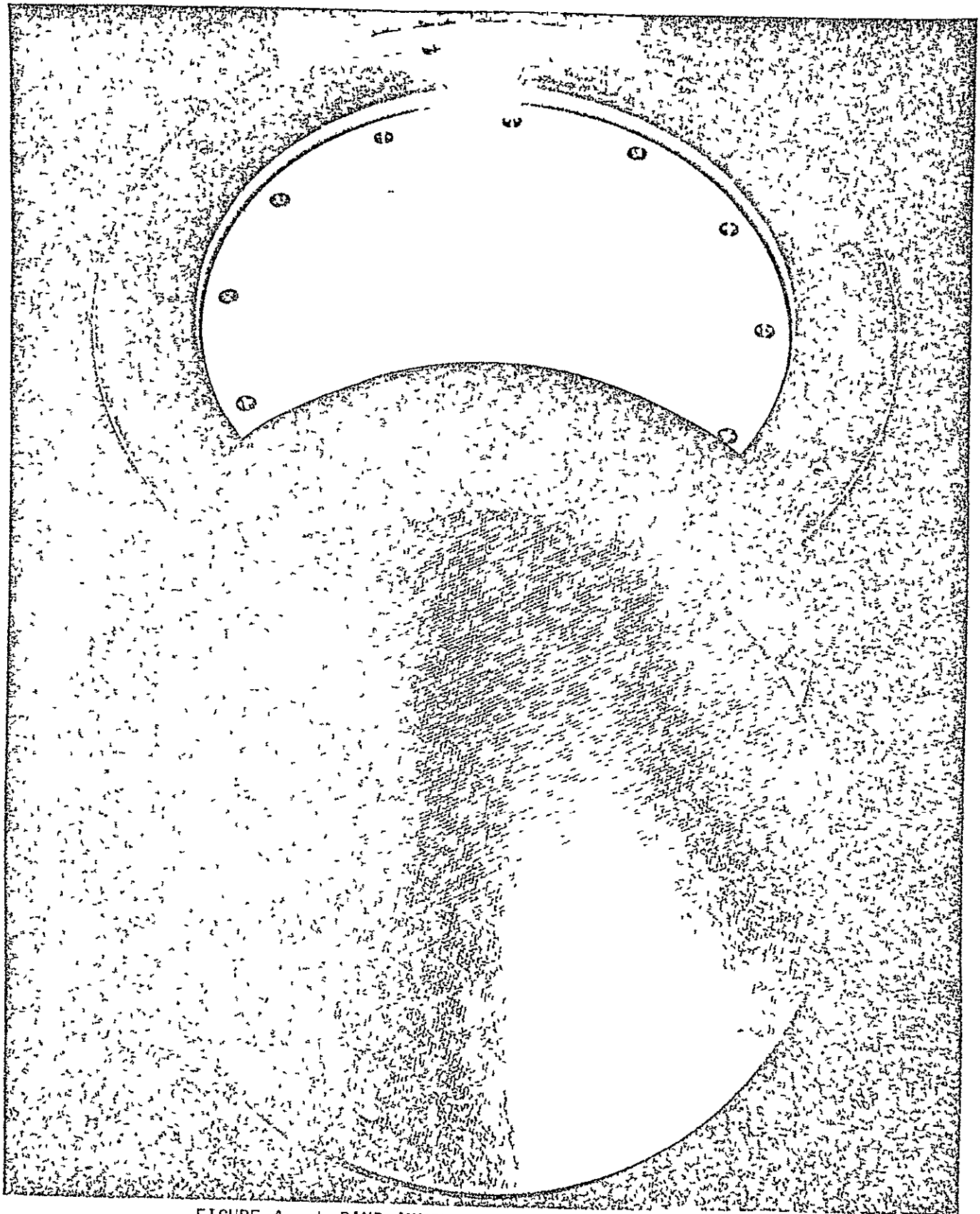

FIGURE 4 - L-BAND ANTENNA IN MOUNTING BRACKET WITH MOISTURE AVOIDANCE PAD AND CARRIER PANEL

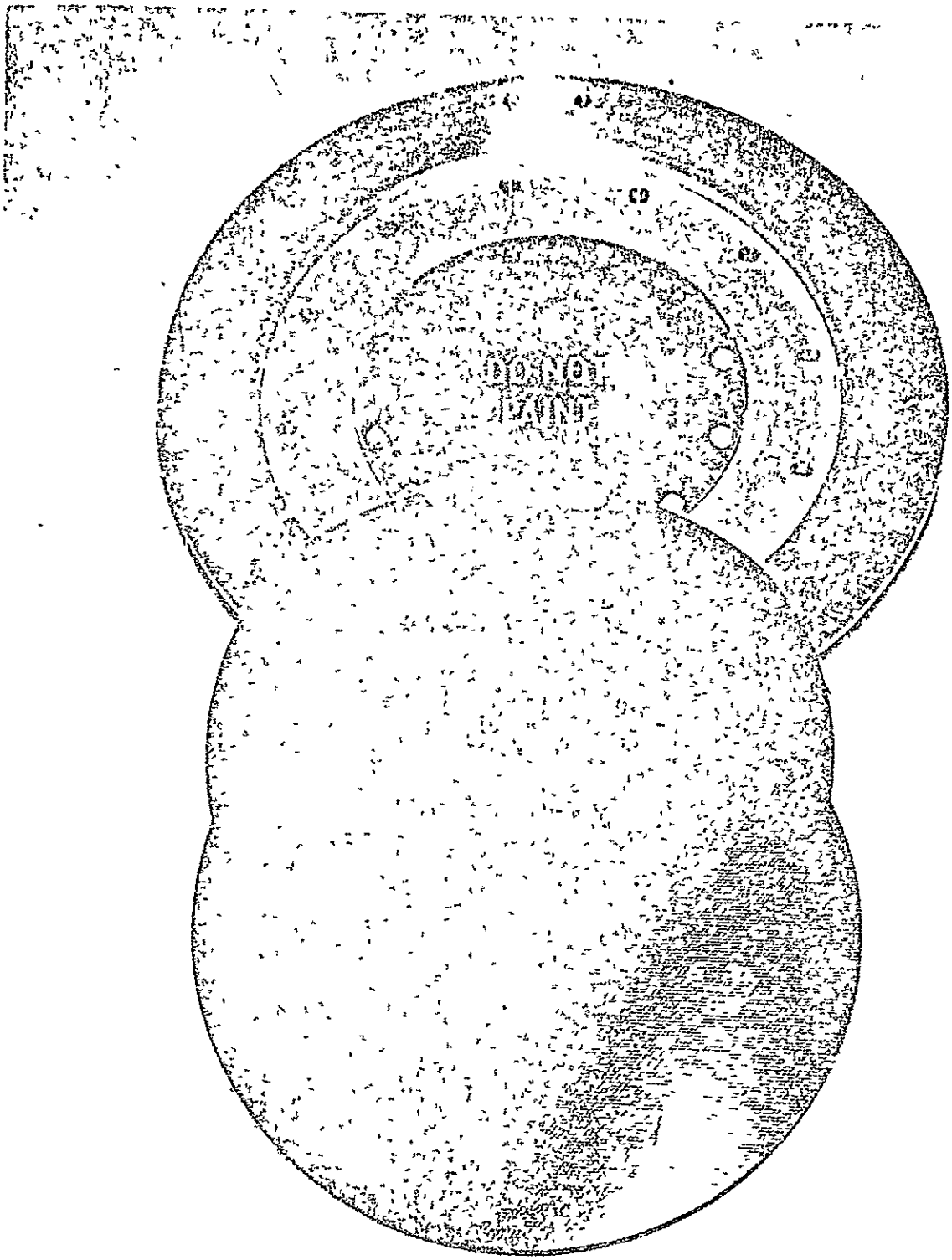

FIGURE 5 - C-BAND ANTENNA IN MOUNTING BRACKET WITH MOISTURE AVOIDANCE PAD AND CARRIER PANEL

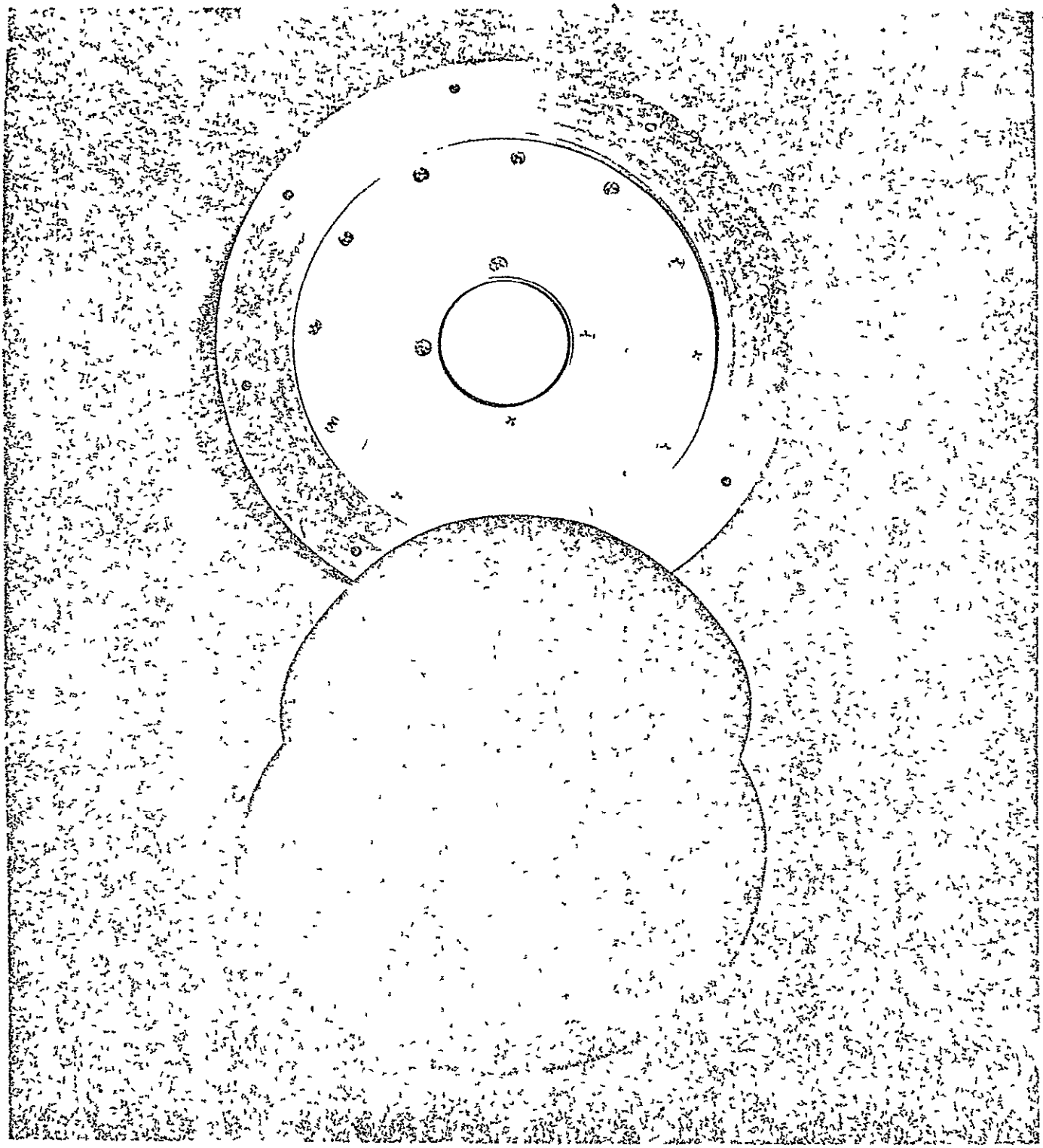

FIGURE 6 - S-BAND ANTENNA IN MOUNTING BRACKET WITH MOISTURE AVOIDANCE PAD AND CARRIER PANEL

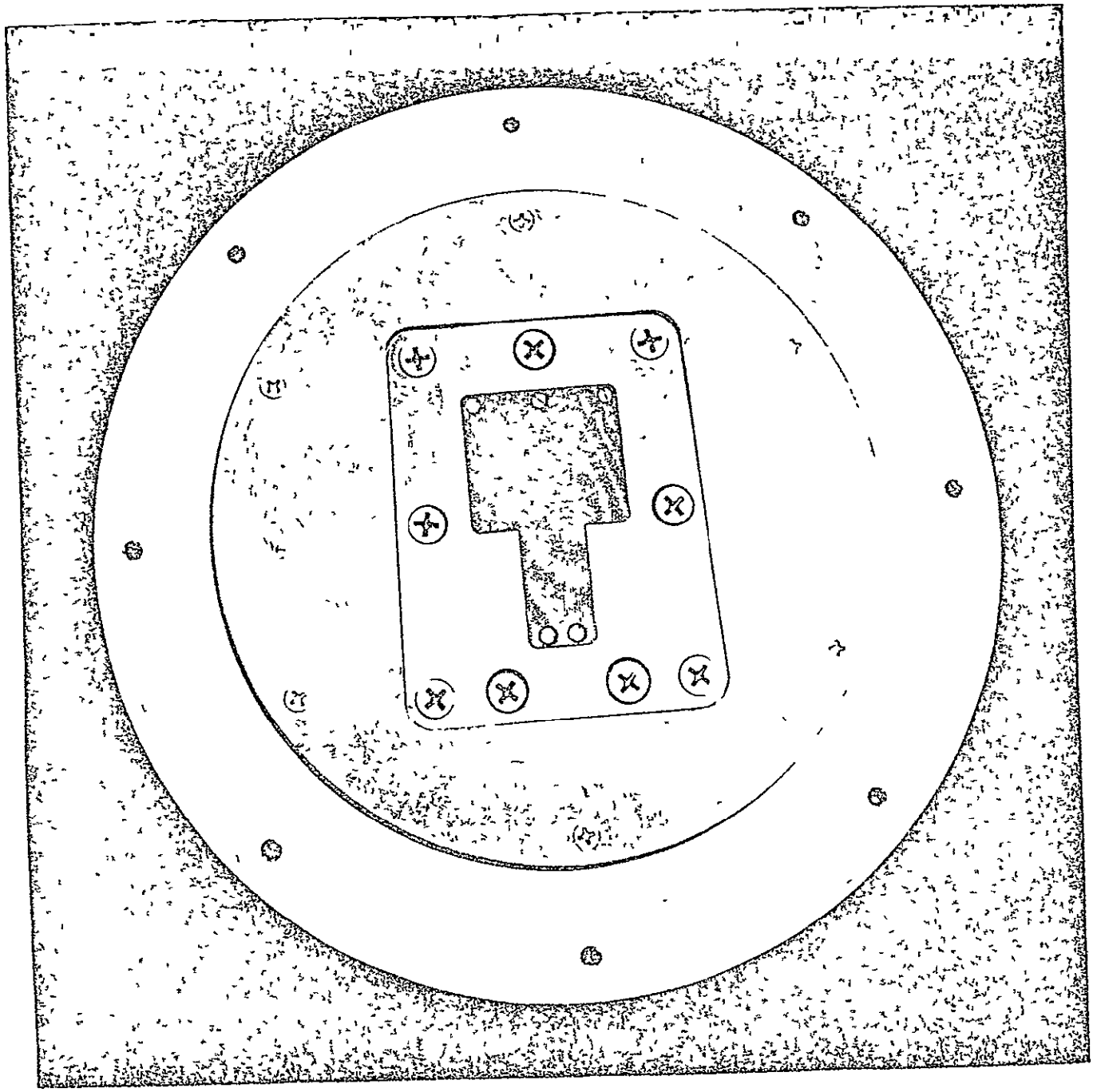

FIGURE 7 - KU-BAND ANTENNA IN MOUNTING BRACKET

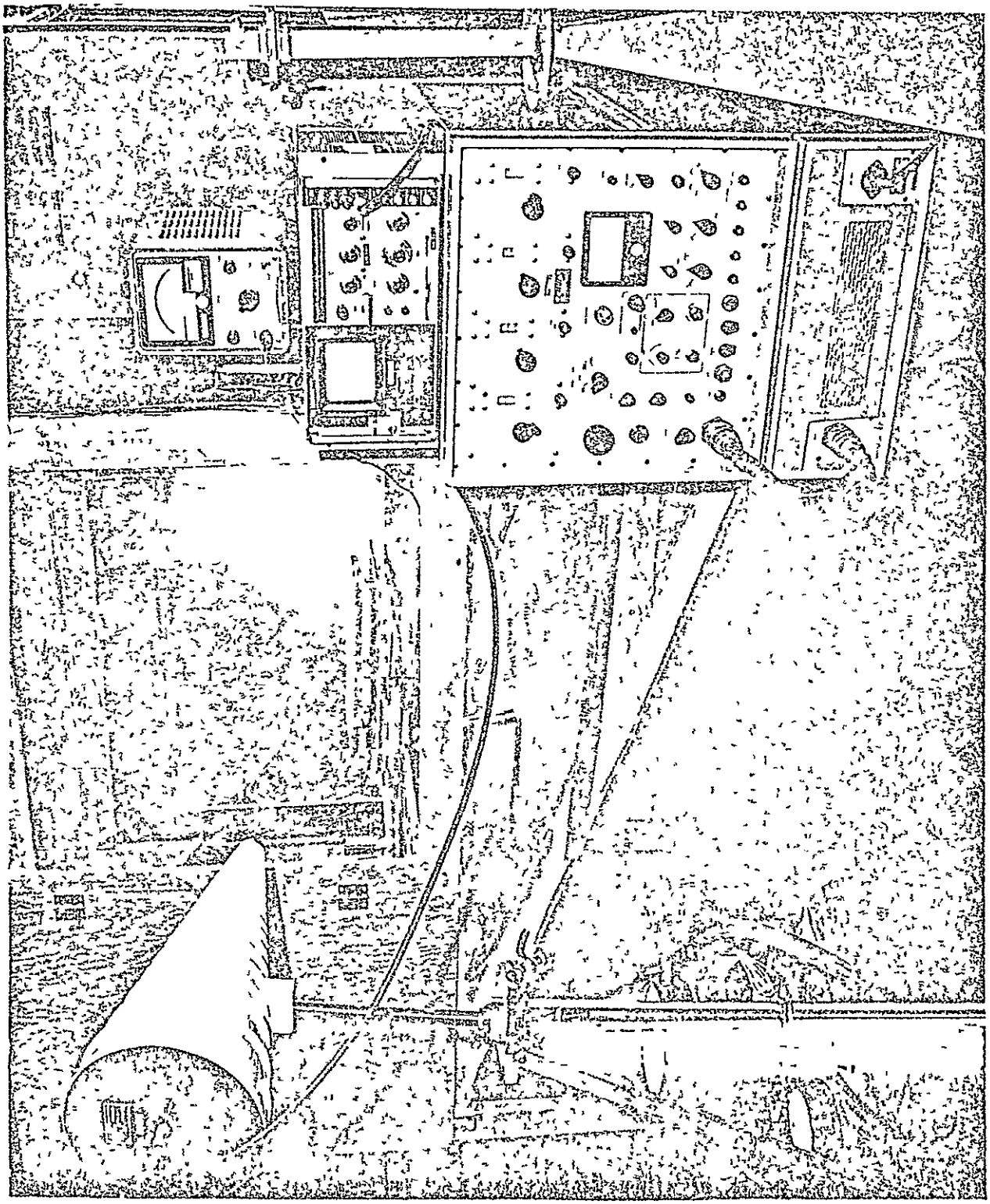

FIGURE 8 - BLOWN DUST TEST SETUP

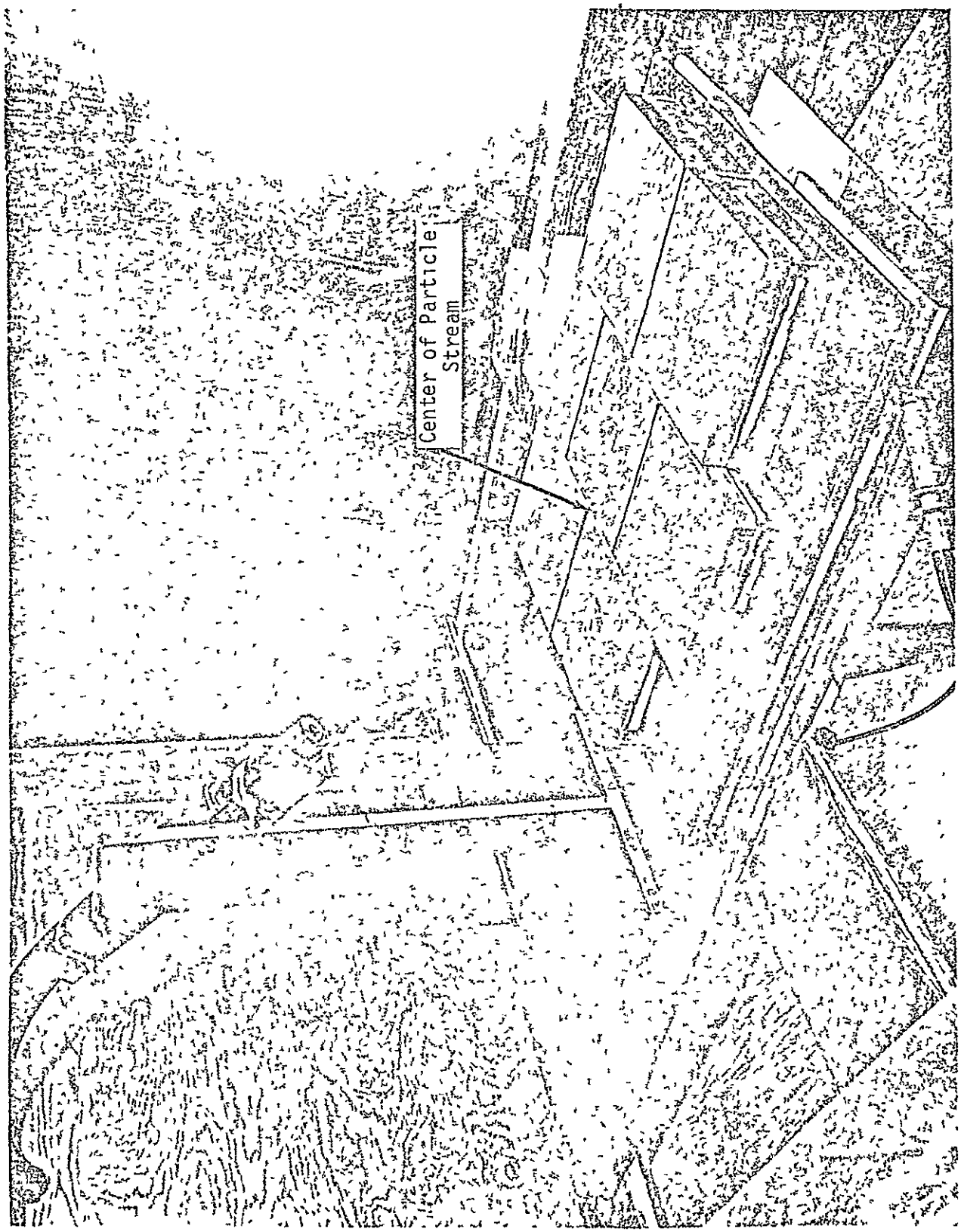

FIGURE 9 - CLOSE-UP OF TPS PANEL INSTALLED IN THE BLOWN DUST TEST SETUP

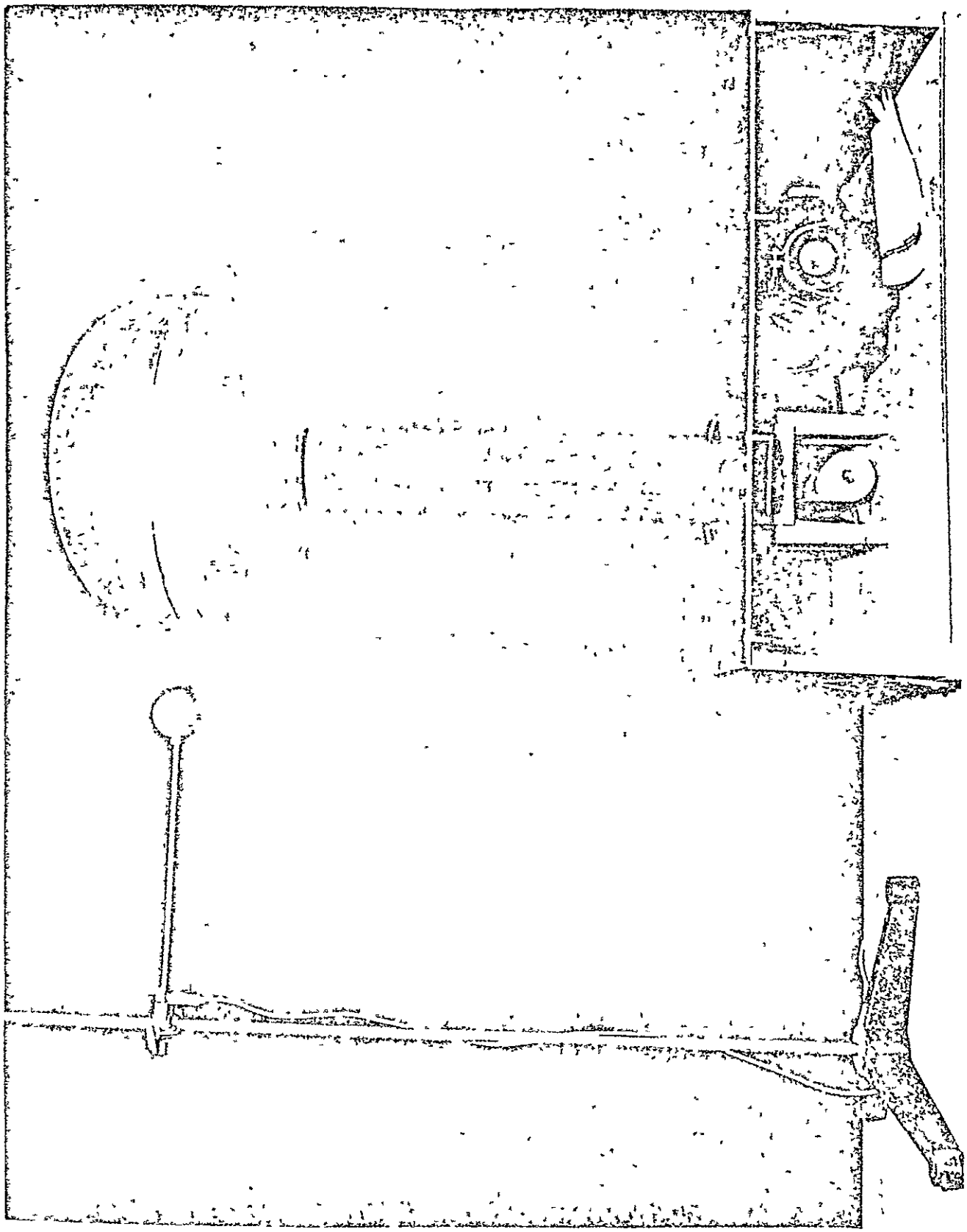

FIGURE 10 - VAN DE GRAAFF GENERATOR TEST SETUP

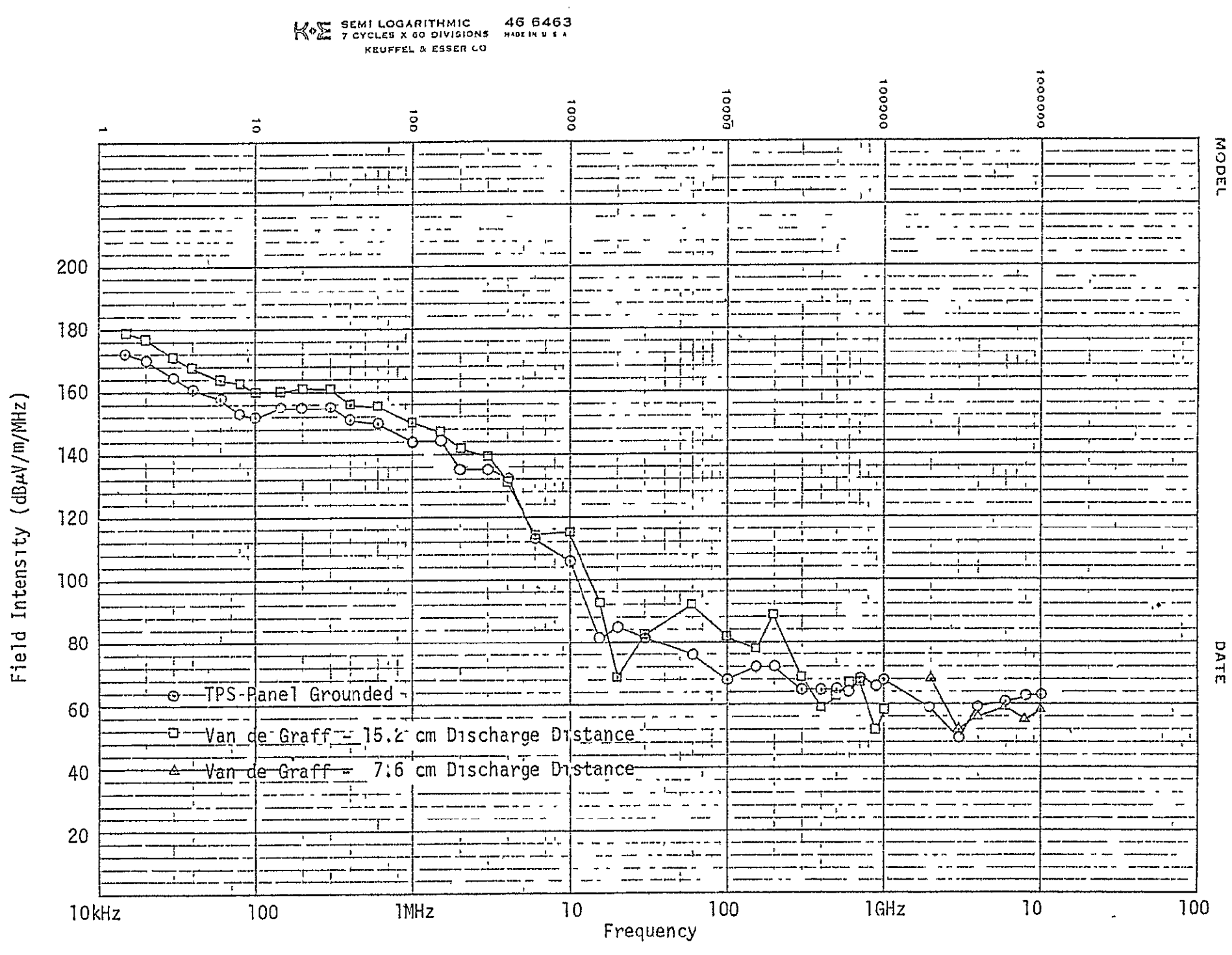

FIGURE 11 - INTERFERENCE LEVELS FOR BLOWN DUST ON TPS AND VAN DE GRAFF TESTS

TABLE 1 - EMI TEST EQUIPMENT

Instrument	Manufacturer	Model	Detector Function	Type of Test	Test Frequency
Interference Analyzer	Fairchild	EMC-25	Peak Peak	Radiated Noise Antenna Noise	14kHz to 1GHz 10MHz, 960MHz
Radio Interference Field Intensity Meter	Stoddart	NM-62B	Slideback Peak Direct Peak	Radiated Noise Antenna Noise	1.94GHz to 10GHz 1GHz to 6GHz
Microwave Receiver/ Ku-Band Mixer	Scientific-Atlanta/ PRD Electronics	1710/616	Signal	Radiated Noise	12.4GHz to 18GHz
Spectrum Analyzer	Hewlett-Packard	8552A, 8555B	N/A	Antenna Noise	10.3GHz to 18.4GHz
Remote Vertical Antenna	Singer	VR-105	N/A	Radiated Noise	14kHz to 100kHz
Vertical Antenna	Empire	VA-105	N/A	Radiated Noise	150kHz to 30MHz
Bi-Conical Antenna	Empire	DM-105-T1	N/A	Radiated Noise	60MHz to 150MHz
Spiral Cone Antenna	Stoddart	93490-1	N/A	Radiated Noise	200MHz to 1GHz
Standard Gain Horn	Scientific-Atlanta	SGH 1.7	N/A	Radiated Noise	1.94GHz
Standard Gain Horn	Scientific-Atlanta	SGH 2.6	N/A	Radiated Noise	3GHz
Broadband Horn	Sylvania	AN-10	N/A	Radiated Noise	4GHz to 10GHz
Standard Gain Horn	Scientific-Atlanta	SHG12-12	N/A	Radiated Noise	12.4GHz to 18GHz

TABLE 2 - CHARGING CURRENT MEASUREMENTS

Material	Charging Current/	
	μamp	μamp/m^2
Aluminum	-0.7	- 220
LI 1500 (single tile)	-5.9	-1800
LI 1500 (7 tile panel)	-8.0	-2500
Quartz	-6.0	-1800
Polyurethane (coated)*	+0.1	+ 31
Window Glass PPG	-3.0	- 930
Pyrex	-3.2	- 990
Plexiglass	-0.5	- 150
Phenolic	-10	-3100
Fiberglass	+0.1	+ 31
Titanium	-1.3	- 400

*Polyurethane coating was Epon 828/Versamid 125; charging current increased to + 0.3μ amps after 1 minute; coating erosion was noted after test.

TABLE 3 - FIELD-INTENSITY DATA

Test Frequency	Blown Dust On TPS (dBμV/m/MHz)			Van de Graff Generator (dBμV/m/MHz)		
		Panel	Panel		Discharge Distance	
(MHz)	Ambient	Grounded	Floating	Ambient	15.2 cm	7.6 cm*
.014	129	172	170	117	179	218
.02	122	170	165	115	177	216
.03	121	165	161	110	171	212
.04	115	161	159	99	168	209
.06	111	158	155	96	164	205
.08	110	153	151	93	163	204
.1	108	152	150	90	160	201
.15	105	155	153	94	160	197
.2	116	155	153	101	161	203
.3	106	155	153	82	161	204
.4	99	151	149	79	156	193
.6	118	150	148	108	155	198
1.0	108	144	142	103	150	186
1.5	114	145	142	79	147	187
2.0	114	135	133	96	142	185
3.0	78	135	129	82	139	180
4.0	83	132	127	83	131	174
6.0	76	113	114	71	114	164
10.0	81	106	104	83	115	165
15.0	65	81	76	53	89	133
20.0	64	85	79	50	69	110
30.0	58	81	79	57	82	134
60.0	53	76	71	46	92	124
100	50	68	63	42	82	113
150	51	72	69	71	78	125
200	57	72	70	72	89	116
300	54	65	60	50	69	107
400	54	65	68	54	59	99
500	58	65	67	52	63	93
600	57	64	65	54	67	104
700	49	69	71	51	67	92
900	51	66	63	47	52	83
1000	50	68	65	49	58	87
1940	27	59	57	27	34	68
3000	33	49	51	33	33	52
4000	45	59	56	42	42	56
6000	45	61	62	45	45	59
8000	50	63	62	49	49	55
10000	55	63	66	54	54	58
12400	55	55	55	55	55	55
14000	51	51	51	52	52	52
15500	52	52	52	52	52	52
18000	54	54	54	52	52	52

*Values occurred on spark discharge only.

TABLE 4 - ANTENNA NOISE TEST DATA AND SHUTTLE RECEIVER SENSITIVITIES

Antenna Type (Operating Frequency, GHz)	Test Frequency (GHz)	Test Bandwidth (MHz)	Test Noise Level		Shuttle Receiver	
			Blown Dust (dBm)	Ambient (dBm)	Bandwidth (MHz)	Minimum Sensitivity (dBm)
L-Band	.01	.05	-85	-112		
(.962 to 1.213)	.96	.5	-56	- 80		
	1.0	5	-67	- 87	1	-90
	1.1	5	-69	- 87		
	1.2	5	-67	- 87		
	2.0	5	-75	- 87		
S-Band	1.5	5	-69	- 87		Lock to
(1.776 to 2.106)	1.78	5	-69	- 87		-121,
	1.94	5	-73	- 87	5	Track to
	2.1	5	-71	- 87		-131
	3.5	5	-73	- 87		
C-Band	2.0	5	-73	- 87		
(4.2 to 4.4)	4.2	5	-72	- 85		
	4.3	5	-67	- 87	10	-80
	4.4	5	-65	- 79		
	6.0	5	-75	- 87		
Ku-Band	10.3	.1	-66	- 66		
(15.412 to 15.688)	15.5	.1	-62	- 62		Angular
	18.4	.1	-63	- 63		-74,
	15.475	.001	-83	- 83	20	DME
	15.500	.001	-83	- 83		-77
	15.525	.001	-83	- 83		